

CALSAGOS: Clustering ALgorithmS Applied to Galaxies in Overdense Systems

D. E. Olave-Rojas¹, [★] P. Cerulo², P. Araya-Araya³, D. A. Olave-Rojas⁴,

¹*Departamento de Tecnologías Industriales, Facultad de Ingeniería, Universidad de Talca, Los Niches km 1, Curicó, Chile*

²*Departamento de Ingeniería Informática y Ciencias de la Computación, Universidad de Concepción, Chile*

³*Departamento de Astronomía, Instituto de Astronomia, Geofísica e Ciências Atmosféricas da Universidade de São Paulo, Cidade Universitária, CEP: 05508-900, São Paulo, SP, Brazil*

⁴*Instituto de Investigación Interdisciplinaria, Universidad de Talca, 1 Poniente 1141, Talca, Chile*

Accepted XXX. Received YYY; in original form ZZZ

ABSTRACT

In this paper we present CALSAGOS: Clustering ALgorithmS Applied to Galaxies in Overdense Systems which is a PYTHON package developed to select cluster members and to search, find, and identify substructures. CALSAGOS is based on clustering algorithms and was developed to be used in spectroscopic and photometric samples. To test the performance of CALSAGOS we use the S-PLUS’s mock catalogues and we found an error of 1% - 6% on member selection depending on the function that is used. Besides, CALSAGOS has a F_1 -score of 0.8, a precision of 85% and a completeness of 100% in the identification of substructures in the outer regions of galaxy clusters ($r > r_{200}$). The F_1 -score, precision and completeness of CALSAGOS fall to 0.5, 75% and 40% when we consider all substructure identifications (inner and outer) due to the function that searches, finds, and identifies the substructures works in 2D and cannot resolve the substructures projected over others.

Key words: galaxies: clusters: general - galaxies: groups: general

1 INTRODUCTION

In the last four decades, several authors (e.g. Dressler 1980, Couch et al. 1998, Kauffmann et al. 2004, Postman et al. 2005, Peng et al. 2010, Jaffé et al. 2016, Cerulo et al. 2017, Olave-Rojas et al. 2018, van der Burg et al. 2020, Lima-Dias et al. 2021) have shown that the environment plays a fundamental role in the evolution of galaxies. In this context, theoretical and observational studies (e.g. Lewis et al. 2002, Poggianti et al. 2006, McGee et al. 2009, Demarco et al. 2010, Jaffé et al. 2016, Cerulo et al. 2017) show that the some physical properties of galaxies are affected by the environment in which these are located and that the environment can trigger processes that drive the evolution of galaxies.

In particular, the observational evidence shows that galaxies in dense environments such as clusters and groups are less star-forming than galaxies in sparse environments (Poggianti et al. 1999, Dressler et al. 1999, Poggianti et al. 2006, Gobat et al. 2008). According to this, galaxy clusters are one the best laboratories to study and understand the

environmental drivers of galaxy evolution. Due to the broad range of densities available in clusters, we can trace the evolution of galaxies through the analysis of galaxy properties from the diversely dense cluster outskirts to the dense cluster cores.

Besides, according to the Λ CDM hierarchical paradigm, galaxy clusters grow and increase their mass through the continuous accretion of less massive structures (i.e. galaxies from the field or groups) or even through the merger with other clusters or filaments (Press & Schechter 1974, Fakhouri et al. 2010, Chiang et al. 2013). In this sense, the study of galaxy properties in the outer regions of galaxy clusters is crucial to understand the connections between galaxy evolution and the formation of their hosting large-scale structures. In particular, several astronomers (Hou et al. 2014, Cybulski et al. 2014, Haines et al. 2015, Olave-Rojas et al. 2018, Just et al. 2019) have focused on the study of the fraction of star-forming galaxies in the outer regions of galaxy clusters. In general these works show that the fraction of quiescent galaxies (i.e. galaxies without star-formation) is always higher in clusters than in the field even at large clustercentric distances ($r \gtrsim 3r_{200}$, e.g. Haines et al. 2015, Olave-Rojas et al. 2018).

[★] E-mail: daniela.olave@utalca.cl

The above results cannot be explained only by models in which quiescent galaxies are accreted directly from the field or by theoretical models in which galaxies quenched their star-formation when they crossed the cluster dark matter halo at r_{200} (Haines et al. 2015). For this reason, some authors (e.g. Fujita 2004, McGee et al. 2009, Vijayaraghavan & Ricker 2013), suggest in their theoretical models that the pre-processing of galaxies (Zabludoff & Mulchaey 1998), is the responsible for the high fraction of quiescent galaxies in the outer regions of galaxy clusters. The pre-processing is a scenario in which galaxies quench their star-formation in galaxy groups before these systems are accreted onto a cluster (McGee et al. 2009, Vijayaraghavan & Ricker 2013, Bahé et al. 2013). In this context, theoretical works (e.g. Vijayaraghavan & Ricker 2013) show that it is possible to detect galaxy groups that were accreted onto clusters as substructures within the three-dimensional distribution of the cluster member galaxies. As Dressler & Shectman (1988) showed, galaxies in substructures retain part of the kinematic information about their progenitor groups.

Motivated by these findings, we have embarked in a project dedicated to the study of the effects of the environment on the evolution of galaxies, particularly focussing on the understanding of the connections between galaxy evolution and the formation of galaxy clusters. By dividing a cluster of galaxies into its main halo and its substructures, one can study the properties of galaxies in these two distinct environments and infer the relevance of pre-processing in shaping the physical properties of galaxies.

The first difficulty to overcome in any kind of observational study of the pre-processing is the accurate detection of substructures and galaxy groups in and around galaxy clusters (e.g. Cohn 2012, Tempel et al. 2017). One observational technique for the identification of substructures is based on the analysis of the X-ray light profile of the Intra Cluster Medium (ICM) where substructures appear as peaks (e.g. Bianconi et al. 2018). However, this method is biased in favour of the most massive and dense substructures within a cluster.

In order to identify low- and high-mass substructures and accreted groups, some authors (e.g. Dressler et al. 2013, Hou et al. 2014, Jaffé et al. 2016, Olave-Rojas et al. 2018, Lima-Dias et al. 2021) use the Dressler-Schectman Test (DS-Test, Dressler & Shectman 1988). This statistical test allows one to determine the probability that a cluster has substructures and also assigns to each galaxy a value that corresponds to the probability of a galaxy to belong to a substructure. Galaxies with high probability to be a part of a substructure have peculiar velocities that deviate from the peculiar velocity distribution of the cluster. It is important to note that: 1) to effectively identify substructures with the DS-Test it is necessary to have a large spectroscopic coverage in the outskirts of the cluster, 2) the substructures identified are preferentially in the cluster outskirts (West & Bothun 1990, Hou et al. 2012, Dressler et al. 2013), and 3) the DS-Test only evaluates whether a galaxy belongs or not to a substructure with a certain probability without returning a list of the substructures of the cluster (Dressler et al. 2013, Jaffé et al. 2013). For the latter task it is necessary to combine the DS-Test output with other techniques based for example on the clustering of data (e.g. Olave-Rojas et al. 2018).

Clustering algorithms are unsupervised machine learning algorithms that were developed to group data points within a sample. So one can apply clustering in the three dimensional space of right ascension, declination and redshift, or in the two-dimensional space of right ascension and declination if spectroscopic redshifts are not available, to detect substructures in clusters of galaxies. One of the most known clustering algorithms is the mixture of Gaussians in which it is assumed that the distribution of galaxies is well reproduced by a collection of Gaussians, with each Gaussian corresponding to a single substructure (e.g. Balestra et al. 2016). Other clustering algorithms are based on the density of the data points in the parameter space. In these cases the clusters are defined as areas of high density separated by areas of low density. In this kind of algorithms the density of the clusters is generally defined based on the number of points and distance between them (e.g. Xu et al. 2019). Due to their simplicity and versatility, in the last decade clustering algorithms have become popular as tools to identify substructures in clusters of galaxies (e.g. Cybulski et al. 2014, Olave-Rojas et al. 2018, Lima-Dias et al. 2021) especially when there is low spectroscopic information.

This paper presents CALSAGOS: Clustering ALgorithmS Applied to Galaxies in Overdense Systems, which is a PYTHON package based on several clustering algorithms developed to select cluster members and to search, find, and identify substructures and galaxy groups in and around galaxy clusters. This package was developed to carry out the analysis presented by Olave-Rojas et al. (2018), and we are releasing it to provide the astronomy community with a tool that can be used for the detection of substructures in cases in which there is limited or no spectroscopic information available. Furthermore, this package can exploit both spectroscopic and photometric redshifts when they are available/measurable, with all the limitations carried with the usage of photometric redshift, as we will discuss in Section 2.2.2. Throughout the paper we adopt a Λ CDM cosmology with $\Omega_{\Lambda} = 0.685$, $\Omega_m = 0.3$ and $h = H_0/100 \text{ km s}^{-1} \text{ Mpc}^{-1} = 0.673$ (Planck Collaboration et al. 2014) in order to be consistent with the mock catalogues (Araya-Araya et al. 2021) used to test CALSAGOS.

In this paper we will recurrently use the terms principal halo, subhalos, and substructures. The principal halo refers to the main body of the cluster. The subhalos correspond to structures smaller than the principal halo that are linked to it; the members of each subhalo are gravitationally linked between them and bounded to its potential well. The substructures are galaxy groups that were accreted into the principal halo and that can be distinguished within the main body of the cluster through the analysis of the velocity and spatial distribution of the galaxies.

The paper is organized as follows. In Section 2 we present and describe CALSAGOS. In Section 3 we present the testing and results of the performance of CALSAGOS. In Section 4 we discuss the performance and limitations of CALSAGOS. Finally, in Section 5 we summarise our main conclusions.

2 STRUCTURE OF CALSAGOS

CALSAGOS was developed in PYTHON version 3.8, using pre-existing modules such as `numpy` version ‘1.21.3’, `astropy` version ‘4.3.1’, `matplotlib` version ‘3.4.3’, `sys`, `math`, `sklearn` version ‘1.0.1’, `scipy` version ‘1.7.1’ and `kneebow` version ‘0.1.1’.

2.1 Modules

CALSAGOS has seven modules that can be used separately or together, depending on user preferences. In each module there are several functions written to estimate different galaxy properties and select cluster members, and/or assign galaxies to substructures. The modules of CALSAGOS are listed below:

(i) `utils`: This module contains a collection of utility functions developed to estimate errors, physical quantities of the clusters, projected distances, and convert units.

(ii) `redshift_boundaries` This module has a collection of functions developed to estimate the central cluster redshift, the velocity dispersion of the cluster, and limits of the redshift distribution, which can be used to select the cluster members.

(iii) `cluster_kinematics` This module contains functions that allow the user to estimate some kinematic properties of a single galaxy cluster.

(iv) `ds_test` contains a collection of functions developed to implement the DS-Test. This module is recommended for use when there are spectroscopic data.

(v) `ISOMER` Identifier of Spectroscopic MemBERS is a module that contains a function to identify spectroscopic cluster members. These are defined as those galaxies with a peculiar velocity lower than the escape velocity of the cluster. This module was developed to carry out the analysis presented in [Olave-Rojas et al. \(2018\)](#).

(vi) `CLUMBERI` CLUster MemBER Identifier is a module that contains a function that identifies cluster members assuming that the sample is well reproduced by a collection of Gaussian. `CLUMBERI` can select spectroscopic or photometric cluster members through a 3D implementation of the Gaussian-Mixture Models (GMM, [Muratov & Gnedin 2010](#)) and using the positions and redshifts of the galaxies.

(vii) `LAGASU` LABeller of GALaxies within SUBstructures is a module that allows one to assign galaxies to different substructures in and around galaxy clusters by using GMM and Density-Based Spatial Clustering of Applications with Noise (DBSCAN, [Ester et al. 1996](#)).

For more details about the different modules and functions please read the help of each one. The webpage of CALSAGOS¹ also provides an example that shows the functioning of the software.

2.2 Clustering Algorithms

The identification of substructures in clusters of galaxies is performed in two steps which are the determination of cluster membership and the identification of substructures in

the two- or three-dimensional spatial distribution of cluster member galaxies. We describe the two steps in this subsection, considering the case in which spectroscopic or photometric redshifts are available and the case in which no redshift information is available. It is important to stress that if we are provided with a catalogue of cluster members it is not necessary to run again the first step.

2.2.1 Members Selection

To select cluster members using the spectroscopic redshifts of the galaxies we have developed `ISOMER`, which is a function that selects cluster members as those objects with a peculiar velocity lower than the escape velocity of the cluster. The escape velocity of the cluster is estimated using the equation published in [Diaferio \(1999\)](#) given by:

$$v_{esc} \approx 927 \left(\frac{M_{200}}{10^{14} h^{-1} M_{\odot}} \right)^{1/2} \left(\frac{r_{200}}{h^{-1} \text{Mpc}} \right)^{-1/2} \text{ km s}^{-1} \quad (1)$$

To use this equation we need to know the M_{200} and r_{200} ² of the cluster. If one only knows M_{200} , r_{200} can be derived using the equation published in [Finn et al. \(2005\)](#):

$$200\rho_c(z) = \frac{M_{cl}}{4/3\pi r_{200}^3} \quad (2)$$

Where $\rho_c(z)$ corresponds to the critical density of the Universe at a particular redshift. Finally, the peculiar velocity of each galaxy is estimated with the following equation published in [Harrison \(1974\)](#):

$$v = c \frac{z - z_{cl}}{1 + z_{cl}} \quad (3)$$

This equation is valid, to first order, for $v \ll c$. Equations (1), (2) and (3) are all implemented in `cluster_kinematics`.

In the practice, to select cluster members all galaxies with a peculiar velocity higher than the escape velocity of the cluster are removed from the sample. Then the velocity dispersion is estimated in this clean sample using the biweight estimator described in [Beers et al. \(1990\)](#) and that is implemented in `astropy`. The error in the velocity dispersion is determined through bootstrap resampling. Finally, the field interlopers are removed by using a 3σ clipping algorithm ([Yahil & Vidal 1977](#)). This approach was developed and implemented in [Cerulo et al. \(2016\)](#) and [Olave-Rojas et al. \(2018\)](#). The uncertainties in the cluster member selection will be discussed in detail in the next section.

When the spectroscopic information is only partially available or not available at all, clustering methods can be adopted to select cluster members and substructures. `CLUMBERI` is a function that uses the GMM implementation of `sklearn` to select cluster members when the spectroscopic and/or photometric redshifts and the positions of galaxies in the sky are available.

GMM is a clustering algorithm that is based on the assumption that the distribution of data points in the parameter space of a sample is well represented by a collection

² M_{200} and r_{200} are respectively the mass and radius of a sphere with a mean density equal to 200 times the critical density of the Universe at the redshift of the cluster.

¹ <https://github.com/dolaver/calsagos/>

of n Gaussian functions, each function representing a cluster. The points in the sample are assigned to a certain Gaussian according to their probability of belonging to it. CLUMBERI requires as input the maximum number N of Gaussians to fit for four different types of co-variances, i. e. *spherical*, *tied*, *diag*, *full*. Thus, for each definition of the covariance matrix, CLUMBERI runs GMM with a number of Gaussians that grows from 1 to N and then uses the Bayesian Information Criterion (BIC, Schwarz 1978) to select the best model. It is important to note that n corresponds to the number of Gaussians that reproduce the sample and N corresponds to the maximum number of Gaussians that we can input to GMM. So, when GMM finds the best model, it selects a number of n Gaussians that is between 1 and N . Finally, the fit of the Gaussians to the galaxy distribution is performed with the Expectation-Maximization (EM, Dempster et al. 1977, Press et al. 2007) algorithm.

CLUMBERI selects cluster members using a 3D implementation of GMM in the space defined by the equatorial coordinates (i.e. R.A. and Dec.) and the redshift of the galaxies. Starting from the initial values of the central position and redshift of the cluster (e.g. those that are reported in a catalogue), CLUMBERI compares the position of the maximum of each Gaussian with the initial position of the centre of the cluster and selects the Gaussian closest (in redshift and position) to the centre of the cluster. Once CLUMBERI has identified the galaxies in this Gaussian, the position of the centre and the redshift of the cluster are updated, and these updated values are used to select cluster members. More specifically, all the galaxies that are at more than 3σ from the updated redshift of the cluster centre are rejected. After the rejection of the outliers CLUMBERI updates the redshift of the cluster and searches for outliers at more than 3σ from the updated value of the cluster redshift. The procedure stops when there are no galaxies at more than 3σ from the cluster redshift. Finally, CLUMBERI estimates the number of cluster members, errors in the estimate of membership, redshift, the velocity dispersion of the cluster, and the uncertainty in velocity dispersion. The errors in the velocity dispersion of the cluster are estimated with bootstrap. The uncertainty in the number of cluster members will be discussed in detail in the next section.

2.2.2 Substructure Identification

When one has a reliable estimation of cluster membership, it is possible to proceed to grouping galaxies within substructures in and around clusters. For this purpose, we developed LAGASU, which is based on two unsupervised Machine Learning algorithms, namely GMM and DBSCAN, both available in `sklearn`,

DBSCAN is a clustering algorithm in which a group is defined as a collection of points within a high-density area separated by low-density areas. To assign the points of the sample to different groups, DBSCAN requires as input the position of the points, epsilon (`eps` or ϵ), and the `min_samples`. The `eps` parameter corresponds to the distance threshold for points to be considered as neighbours: all points at distances shorter than `eps` from a point are its neighbours. `min_samples` corresponds to the minimum number of neighbours that a point must have within `eps` to be considered as member of a real group. All points outside the

identified groups are considered as noise (for further details please see Section 3 of Ester et al. 1996)

The LAGASU module has two functions, namely `lagasu` and `lagasu_dbscan`. The `lagasu` function assigns galaxies to substructures using GMM and DBSCAN. `lagasu` first uses GMM to model the redshift distribution of galaxies with a mixture of n Gaussians. The best number of Gaussians is determined as in CLUMBERI, using the BIC. Afterwards the redshift range of cluster members is sliced according to the width of the Gaussians into n bins. `lagasu` automatically runs DBSCAN in each redshift bin to detect substructures in the projected distribution of the galaxies and assigns galaxies to the substructures encountered. The `lagasu_dbscan` function assigns galaxies to different substructures using only DBSCAN.

If the user has access to spectroscopic data we suggest using `lagasu` because DBSCAN only works in the two-dimensional space of galaxy coordinates. We recommend this since there exist cases in which two galaxies are close in projection but far in redshift. However, if the user has only access to the photometric data we recommend `lagasu_dbscan` because the errors in photometric redshift may be high. For instance, in the case of S-PLUS Molino et al. (2020) found that the estimated z_{phot} have a precision of 3% for galaxies with $z < 0.5$, while Balogh et al. (2021) reports an accuracy of 5% in the Gemini Observations of Galaxies in Rich Early ENvironments (GOGREEN) survey at $0.8 \leq z < 1.5$. As a comparison, the precision of the spectroscopic redshifts in GOGREEN varies between $5 \cdot 10^{-4}$ and $2 \cdot 10^{-3}$.

It is important to note that we do not use GMM to identify the substructures because this algorithm assigns all galaxies to one substructure/group. So there could exist a case in which two galaxies very distant spatially are assigned to the same group. DBSCAN, on the other hand, does not assign all galaxies in the sample to one group (Ester et al. 1996), and galaxies that are not assigned to a substructure are classified as “noise” and assigned to the principal halo of the cluster.

We remark that GMM and DBSCAN are two clustering algorithms, and therefore these tools cannot be used to automatically distinguish between the principal halo and the substructures. All structures are classified as groups. For this reason we suggest the following criterion: when having a spectroscopic sample, the group nearest to the cluster centre should be considered as the principal halo. When only photometric data are available, all groups within a projected distance of r_{200} from the cluster centre should be considered as part of the principal halo. This implementation is done in the `test.py` published on the web-page of CALSAGOS.

Finally, if the user has access to the spectroscopic data, they can first run `ds_test` over the sample of cluster galaxies and then `lagasu`. This with the aim of finding substructures that have kinematic deviations with respect to the cluster.

3 TESTING THE PERFORMANCE OF CALSAGOS

3.1 Data: Mock galaxy catalogue

To test the performance and quantify the accuracy of CALSAGOS, we use the same mock catalogue created for Werner et al. (2022a), who similarly probed the galaxy

cluster detection in the Data Release 1 (DR1) of the Southern Photometric Local Universe Survey (S-PLUS, Mendes de Oliveira et al. 2019). The lightcone, constructed with the techniques in Araya-Araya et al. (2021), has a projected area of 324 deg² and goes up to $z \sim 0.5$. Here we briefly describe its construction for completeness.

The synthetic galaxies of this mock come from applying the L-GALAXIES semi-analytical model (SAM, Henriques et al. 2015) to the Millennium Run (MR) simulation (Springel et al. 2005) scaled to the *Planck* 1 cosmology (Planck Collaboration et al. 2014) (using the Angulo & White 2010 algorithm, included in the SAM source code). The cosmological redshifts are attributed to each galaxy assuming that sources at comoving distances $d_c(z_i) \leq d_{c,gal} \leq d_c(z_i) + 30$ kpc are at the same redshift z_i . Afterwards, the “observed” redshifts are computed by considering the peculiar motions of the galaxies along the line of sight. Finally, following Kitzbichler & White (2007), the celestial coordinates, namely right ascension and declination, are obtained.

The spectro-photometric properties of the modelled galaxies were obtained following the *post-processing* approach described in Shamshiri et al. (2015). This consists in using the star formation history (SFH) arrays of each galaxy (L-GALAXIES output) whose bins store information about stellar masses and metallicities produced between two cosmic times for the following baryonic components: disk, bulge, and intra-cluster medium (ICM). SFH arrays have as many as 20 times (age) bins, depending on the simulation snapshot. For a description of the binning algorithm, see Shamshiri et al. (2015). The sum of disk and bulge SFH arrays can represent the whole stellar component of the modelled galaxies, where each bin can be associated with a simple stellar population and have a spectral energy distribution (SED). The used SED templates are from the Maraston (2005) stellar synthesis population models, assuming a Chabrier (2003) initial mass function (IMF). Over the galaxy component SEDs (sum of all SFH bin SEDs) it is applied the dust extinction model following the approach used by De Lucia & Blaizot (2007), Henriques et al. (2015), Shamshiri et al. (2015), Clay et al. (2015). Then, the final galaxy SED is the sum of both bulge and disk components after the dust correction. Apparent magnitudes were computed for the five S-PLUS broad-bands (u , g , r , i , and z filters), by placing each galaxy SED in the observer-frame, according to its “observed” redshift.

3.1.1 Simulated clusters and their substructures

We did not know a priori which galaxies are cluster/group members. To identify them, we correlated the mock data with a catalogue with dark matter halo information. The latter was obtained from the Virgo-Millennium³ database. Here, as well as in Werner et al. (2022a), we defined the simulated clusters as all primary dark matter halos with $M_{200} \geq 10^{14} M_{\odot}$. In practice (following the database notation), from the MPAHaloTrees.MRscPlanck1 table, we selected all halos with `haloId = firstHaloInFOFgroupId` and `m_crit200 $\geq 10^{14} M_{\odot}$. Notice that, at this point, the first`

condition would select just galaxies in the main cluster halo. We estimated the central Right Ascension (R.A.), Declination (Dec.), and redshift of each cluster as the median position of the galaxy members in its main halo.

At this point, to identify the galaxies in subhalos linked to a particular cluster with `haloId = i` in the mock, again from the Virgo-Millennium database, we extracted all the dark matter halos with `firstHaloInFOFgroupId = i`. By running this search iteratively for all galaxy clusters in the mock, we finally obtained a catalogue with all bounded subhalos and thus galaxies in substructures.

In our implementation of CALSAGOS, we defined a substructure/group as a collection of at least three neighbouring galaxies. For this reason, we removed all those subhalos in the mock with two or fewer members. To test the performance of CALSAGOS we used 200 halos in the mass range $14.7 \leq \log(m_{200}/M_{\odot}) \leq 15.5$ and in the redshift range $0.038 \leq z \leq 0.575$.

3.2 Initial Configuration

In the test.py available in the CALSAGOS repository, a group/substructure is defined as a collection of at least three neighbouring galaxies. This is implemented by setting the parameter `n_galaxies` (or `min_samples`) to 3. However, the user can set this parameter as they prefer as long as its value is greater than 1. The `eps` parameter was determined following the approach suggested by Ester et al. (1996) and Rahmah & Sitanggang (2016). In practice, we estimated the `eps` in each cluster by measuring the distance of each galaxy to its K-Nearest Neighbour (KNN), in our case $K = 3$ since we set `n_galaxies = 3`. Then we sorted the distances in ascending order and selected the `eps` as the point of maximum curvature which was determined through an automated procedure that uses the functions `calc_knn_galaxy_distance` and `best_eps_dbscan` from the module `utilis` of CALSAGOS. In Figure 1 we can see the plot of the sorted KNN-distance for a selected random halo from the S-PLUS mock catalogue (identified as ID26 in our clean catalogue) using $K = 3$. As it is mentioned above, we selected the `eps` as the distance in which the plot has its maximum curvature. This value is represented by a red dashed line in the plot. All galaxies with a KNN-distance above the red line are considered to be noise and all galaxies below this value are assigned to some substructure.

We set to 15 the maximum number of Gaussians that can be fitted in CLUMBERI and LAGASU. We tested the performance of CALSAGOS setting the maximum number N of Gaussians to be fitted in CLUMBERI and LAGASU to values varying from 5 to 30 in steps of 5, and we found similar values of the BIC regardless of the number of Gaussians used. The user can set the parameter N to the same number in both CLUMBERI and LAGASU because in both functions the value of n Gaussians is determined with the BIC in an independent way.

We have tested the performance of `lagasu` and `lagasu_dbscan` and found the same results for both approaches. For this reason, hereafter LAGASU corresponds to the `lagasu` function.

³ <http://gavo.mpa-garching.mpg.de/MyMillennium/>

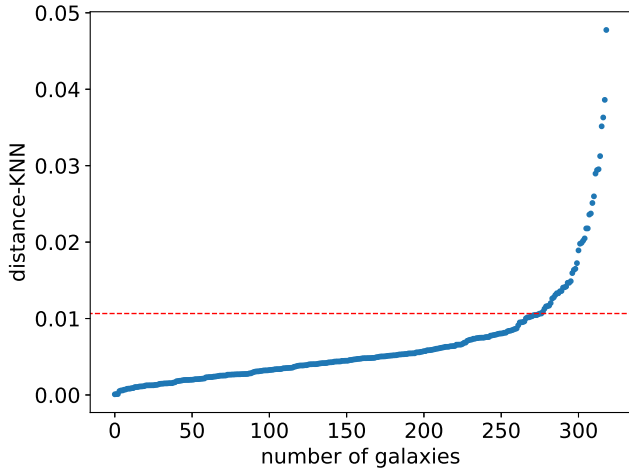


Figure 1. Sorted distance-KNN graph for the sample of the halo ID26 in our clean S-PLUS mock catalogue using $K = 3$. The horizontal red dashed line corresponds to the threshold value of the distance between galaxies. All galaxies with a higher distance-KNN value are considered to be noisy and all other galaxies are assigned to some substructure.

3.3 Uncertainties in the performance of CALSAGOS

To estimate the error on our cluster member selection we ran CALSAGOS in the sample defined in Section 3.1 and we estimated the relative difference between the members of the principal halo in the mock and the members selected by using CLUMBERI or ISOMER. Then we estimated the median of the distribution of the relative differences.

To quantify the performance of LAGASU in the selection of substructures we estimated the F_1 -score (Van Rijsbergen 1979) which allows one to quantify the accuracy in the analysis of binary classification. Our method for the detection of substructures determines whether a galaxy belongs or not to a substructure, so it can be interpreted as a binary classification problem in which we are classifying galaxies into main cluster members and substructure members. CALSAGOS addresses this problem with unsupervised learning, which does not allow one to determine the numbers of false negatives and false positives. However, we chose to test our software on the S-PLUS mock catalogue in which the positions, redshifts and structures of the dark matter halos are all known. This sample provides us with a ground truth against which we can test the performance of the clustering procedures implemented in CALSAGOS; therefore, the F_1 -score can be used in this case to quantify the accuracy of our method for selecting substructures in clusters of galaxies.

The F_1 -score quantifies the quality of the performance of LAGASU as the number of true positive identifications divided by the sum of the number of true positive identifications and the number of total false identifications (i.e. the false negative plus the false positives). This corresponds to the harmonic mean of precision and recall. The F_1 -score is defined as:

$$F_1 = \frac{t_p}{t_p + \frac{1}{2}(f_p + f_n)} \quad (4)$$

where t_p corresponds to the *true positive* identifications, f_p is the *false positive* identifications and f_n corresponds

to the *false negative* identifications. The true positives are substructures identified by LAGASU that correspond to subhalos in the mock catalogue. False positive identifications are substructures that were identified by LAGASU but do not correspond to subhalos in the mock catalogue. Finally, false negative identifications correspond to subhalos that were not identified as substructures by LAGASU. The values of the F_1 -score range from 0 to 1, where 1 corresponds to a perfect classification and 0 means that there is total disagreement between the true and the assigned classes. In addition, the precision or purity of LAGASU was defined as:

$$P = \left(\frac{t_p}{t_p + f_p} \right) 100\%, \quad (5)$$

where P ranges from 0 to 100% and the completeness or recall was defined as:

$$C = \left(\frac{t_p}{t_p + f_n} \right) 100\%. \quad (6)$$

C also ranges between 0 and 100%.

3.4 Results

Using the initial configuration described in Section 3.2 we estimate an error of 1% and 6% in the member selection when we use CLUMBERI and ISOMER, respectively. This difference in the errors is due to ISOMER always selecting fewer cluster members than CLUMBERI. Despite the difference in the number of members obtained with these two functions, when we applied LAGASU over the sample of cluster members, the output was the same regardless of using CLUMBERI or ISOMER.

When we consider all substructures (inner and outer) we obtain a F_1 -score of 0.5, a precision of 75% and a completeness of 40%. When we analyse the type of identifications we find that 64% of subhalos are false negatives. Therefore, we are not able to identify the 64% of the subhalos. This is due to the fact that there is information in 3D that we have not considered. However, 73% of our identifications are true positives (i.e. subhalos that are identified as substructures). These results are mainly due to the fact that LAGASU cannot identify substructures projected over others or over the main cluster, because this module is based on clustering algorithms that work in the two-dimensional coordinate space.

For the reason mentioned above we analyse the performance of LAGASU only considering the outer substructures (i.e. substructures outside $1 \times r_{200}$ from the cluster centre), and we obtain a F_1 score of 0.8, a precision of 85% and a completeness of 100%. When we analyse the type of identifications, we find that 85% of them are true positives. Furthermore, when considering only the outer substructures, none of the subhalos are false negatives. In other words, all subhalos in the outer regions of the cluster are identified as substructures. On the other hand, when we analyse the performance of LAGASU only considering the inner substructures (i.e. substructures within $1 \times r_{200}$ from the cluster centre) we obtain a F_1 -score of 0.4, a precision of 80% and a completeness of 30%. In this case, the 80% of our identifications are true positives and the 70% of the subhalos are false negatives.

The F_1 and the percentages of true positive and false

negative were obtained by estimating each value for each cluster and then deriving the median of the distribution of each of these values for the whole sample. To estimate the error in the number of members of the substructures we used the same approach used to estimate the error in the cluster members, and we found 30% and 20% when considering all and only the outer substructures, respectively.

In Figure 2 we present the output of CALSAGOS for the halo ID26. In the left panel we show the cluster member selection and substructure identification. In this example cluster members were selected with CLUMBERI. According to the S-PLUS mock catalogue, this halo has 319 members and 16 subhalos with 3 or more members. CALSAGOS detects 319 ± 3 members and 11 substructures, which were defined using the criteria for the spectroscopic sample. In the right panel of Figure 2 we show the halo and subhalos according to the information taken from the mock catalogue. The true positive substructures in the left panel have the same colour of the corresponding subhalo in the right panel. Instead, false positive substructures and false negative subhalos are coloured with different colours. Finally, galaxies that are part of the cluster (or principal halo) but are not part of a substructure (or subhalo) are coloured grey.

The S-PLUS mock catalogue contains the halos ID4 and ID5 that are very close to each other in position and redshift (see Table 1). When we plot the members of these halos (see left panel of Figure 3) we can observe that one halo overlaps with the other as if the halos were merged. Due to this fact, regardless of whether we use CLUMBERI or ISOMER to select cluster members of one of these halos, we always select both halos as if they were one (see middle and right panel of Figure 3 and Table 1). Therefore, we find an error of 70% when we selected members using ISOMER and an error of 130% when we select members using CLUMBERI. Furthermore, when we run LAGASU over our catalogue of members obtained with CLUMBERI for these halos, we obtain a F_1 -score of 0.2 and 0.1 for halo ID4 and ID5, respectively, a precision of 55% and 20% for halo ID4 and ID5, respectively and a completeness of 10% for both halos. These results are considering all substructures (inner and outer).

However, if we compared our member selection with the combined halos (i.e. ID4 + ID5) as if they were a single halo, we obtain an error of 0% in the member selection with CLUMBERI and ISOMER. Additionally, when we compare the results obtained with CLUMBERI and LAGASU for the halos ID4 and ID5 with the combined halos we obtain a F_1 -score of 0.1, a precision of 55% and a completeness of 7% for the halo ID4, while for halo ID5 we obtain a F_1 -score of 0.3, a precision of 70% and a completeness of 20%.

When we run only LAGASU over the catalogue with the members of halos ID4 and ID5 taken from the mock we obtain for halo ID4 a F_1 -score of 0.4, a precision of 70% and a completeness of 25%, while for ID5 a F_1 -score of 0.3, a precision of 70% and a completeness of 20%. Finally, we run LAGASU on a catalogue with the members of the combined halos and obtain a F_1 -score of 0.6, a precision of 70% and a completeness of 50%.

In order to discern if there is a bias due to colour or magnitude in the selection of cluster members and the detection of substructures with CALSAGOS, we used the apparent magnitudes in the mock catalogue (see Section 3.1) to obtain the $(g - r)$ colours of the mock galaxies and investigate any

difference between the colour distributions of the subhalo galaxies and the galaxies in the main halo and between the substructure galaxies and the galaxies in the main cluster. Figure 4 shows the $(g - r)$ versus r colour-magnitude diagram (CMD) for the halo ID26. In the left panel of Figure 4 we present the cluster members and subhalos taken from the mock and in the middle and right panels we show the cluster members and substructure identification using CLUMBERI+LAGASU and ISOMER+LAGASU, respectively.

Furthermore, in Figure 5 we present the CMD for the halo ID26, highlighting the true positive (green crosses), false positive (blue crosses), and false negative (red crosses) in our substructure identification. We also present the CMD for all substructures (left panels), outer substructures (middle panels), and inner substructures (right panels). In the top panels cluster members are selected using CLUMBERI, while in the bottom panels they are selected with ISOMER.

With the aim to discern if actual substructure galaxies follow the colour distribution of the cluster members, we perform the Kolmogorov-Smirnov Test (KS Test, Kolmogorov 1933, Smirnov 1948) to compare the colour distribution between the cluster members and substructure members. We use the implementation of the test contained in `ks_2samp` (Hodges 1958) from the PYTHON module `scipy`. We compare the colour of subhalo galaxies with the colours of cluster members in the mock, and we find a p-value of 0.75. When we compare the colours of the galaxies in substructures with the colours of the cluster members selected with CLUMBERI and ISOMER we find a p-value of 1 and 0.2, respectively.

When we run the KS test to compare the colour distributions of all substructures with our member selection we find a p-value of 1, 0.6 and 0.3 for the false negative, false positive and true positive identifications, respectively. When we compare the colour distribution of the galaxies in the outer substructures with that of galaxies in the main cluster we find a p-value of 0.7. Finally, when we perform the comparison for the galaxies in the inner substructures we find a p-value of 0.6, 0.6 and 0.07, for the false negative, false positive and true positive, respectively. In all cases, the p-value is greater than 0.05 for a 95% confidence level. We can conclude that there is no difference and therefore no induced bias in the colour distribution of galaxies in substructures.

Finally, to analyse the performance of CALSAGOS as a function of the different redshift definitions available, we performed the following tests on the halo ID26: i) we selected cluster members, and we identified substructures using the spectroscopic redshifts; ii) we selected cluster members, and we identified substructures using the photometric redshifts; iii) we identified substructures using only the projected positions (R.A. and Dec.). We used LePHARE (Arnouts et al. 1999, Ilbert et al. 2006) to estimate the photometric redshifts in halo ID26, and the results of this test are summarised in Table 2.

Cluster members were selected using CLUMBERI, obtaining 319 ± 3 and 400 ± 4 cluster members using z_{spec} and z_{phot} , respectively. Table 2 shows that the precision of CALSAGOS in identifying substructures falls by 3% for all substructures, 25% for outer substructures and 22% for inner substructures when we use z_{phot} . We expected the worst precision when we only used R.A. and Dec.; however, it can be seen that we obtain the same precision as when using z_{spec} . We argue that this could be a consequence of the fact

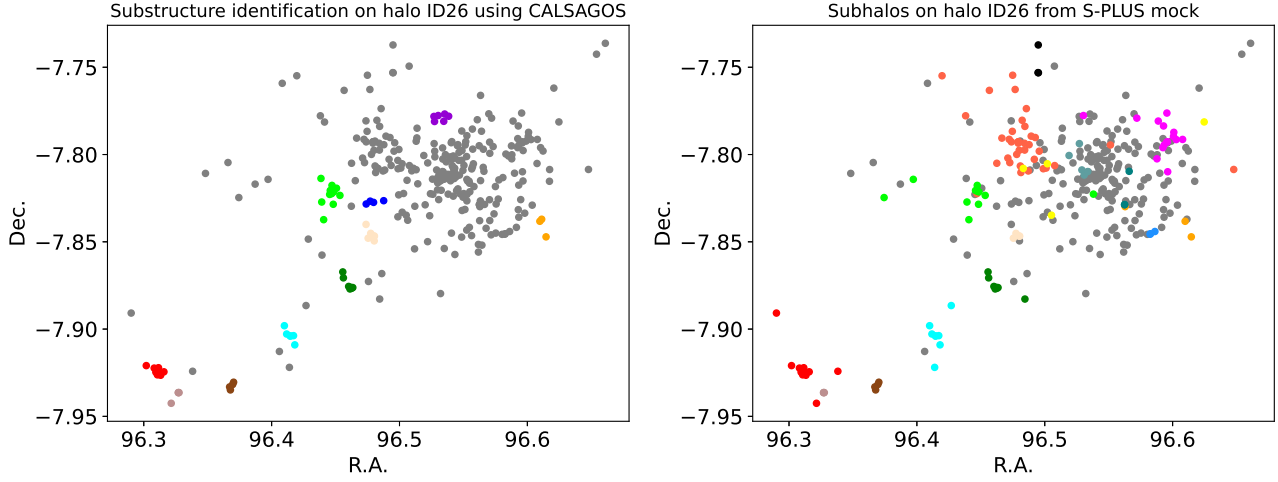


Figure 2. Left panel: substructure identification after running CALSAGOS in the halo ID26 from the S-PLUS mock. Right panel: subhalos in the ID26 halo. According to the S-PLUS mock, the selected halo has 16 subhalos with 3 or more members. With CALSAGOS we identified 11 substructures in this halo. In both cases galaxies in the principal halo are plotted with grey dots and galaxies in subhalos/substructures are plotted with dots of different colours. Galaxies with the same colours in both panels correspond to the same substructure/subhalos.

Table 1. Member identification halos ID4 and ID5

Halo	R.A. (J2000.)	Dec.	z	mass $\log(m_{200}/M_{\odot})$	members ^a	subhalos ^b	members ^c	substructures ^d	members ^e	substructures ^f
ID4	98:26:22.04	06:39:25.73	0.454	15.21	682	51	1185 ± 12	11 ± 2	1129 ± 11	23 ± 5
ID5	98:30:06.98	06:38:24.94	0.455	15.19	503	33	1190 ± 12	21 ± 4	1133 ± 11	47 ± 9

^a number of members according to the mock catalogue

^b number of subhalos with three or more members taken from the mock catalogue

^c number of members obtained using CLUMBERI

^d number of all substructures (inner and outer) obtained using LAGASU after selecting cluster members with CLUMBERI

^e number of members obtained using ISORMER

^f number of all substructures (inner and outer) obtained using LAGASU after selecting cluster members with ISOMER

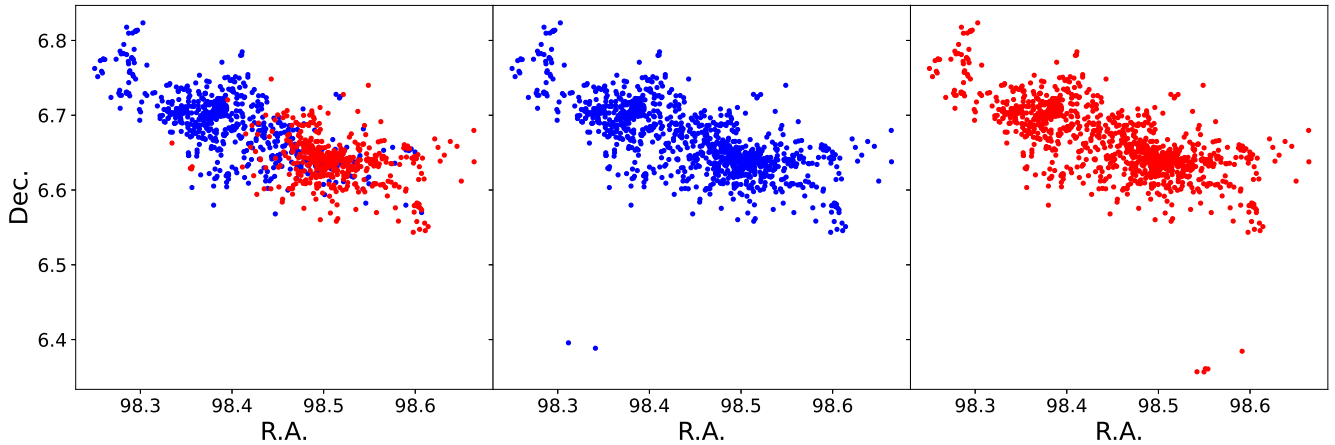


Figure 3. Left panel: blue points represent the members of halo ID4 taken from the mock. This halo has 682 members. Red points represent the members of halo ID5 taken from the mock. This halo has 503 members. Middle panel: all blue points correspond to the members of halo ID4 selected using CLUMBERI. Right panel: all red points correspond to the members of halo ID5 selected using CLUMBERI. We obtained 1185 and 1190 members for the halos ID4 and ID5, respectively.

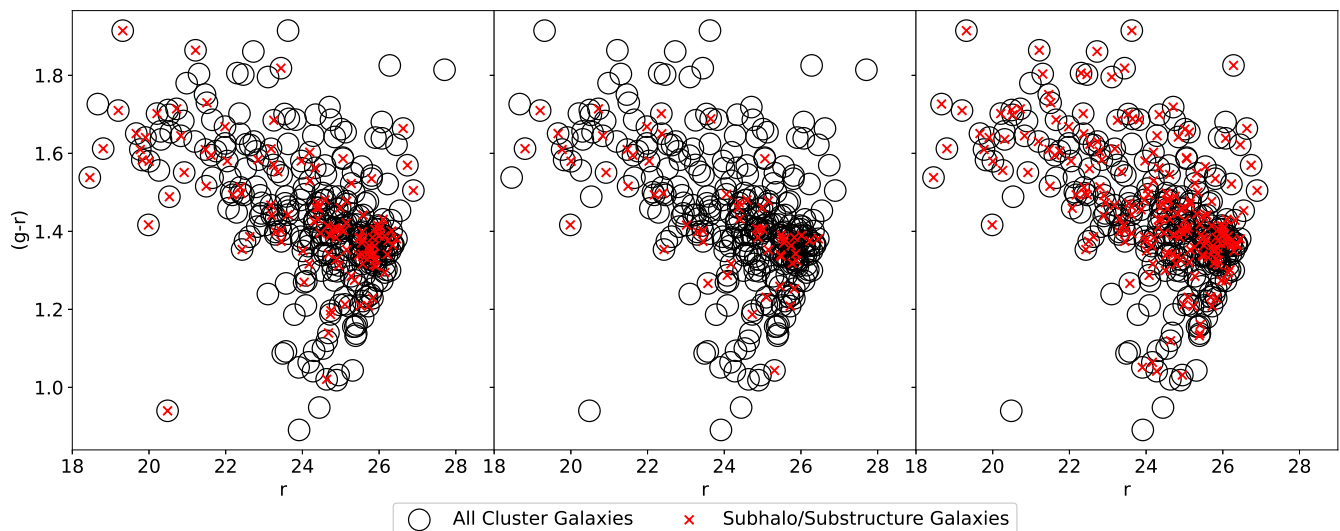


Figure 4. Colour–magnitude diagrams of the halo ID26. The colours are measured in the g and r S-PLUS broad bands (see Section 3.1). Cluster member galaxies are plotted with open black circles and galaxies in substructures are plotted with red crosses. Left panel: cluster members and subhalos of the halo ID26 taken from the mock. Middle panel: cluster members of halo ID26 was selected using CLUMBERI and substructure identification was done using LAGASU. Right panel: members of halo ID26 selected using ISOMER and substructure identification was done using LAGASU.

Table 2. Performance of CALSAGOS on halo ID26 as a function of redshift type

	z_{spec}			z_{phot}			without redshift		
	all	outer	inner	all	outer	inner	all	outer	inner
F ₁ -score	0.67	1	0.53	0.86	0.8	0.64	0.67	1	0.53
Precision	82%	100%	80%	79%	75%	58%	82%	100%	80%
Completeness	56%	100%	40%	94%	86%	70%	56%	100%	40%

that to perform this experiment we selected the halo and not a light cone. So, in this case the mock galaxies seen in projection coincide with the actual members of halo ID26.

3.4.1 CALSAGOS on real data

The first version of CALSAGOS was probed in two real clusters at $z \sim 0.4$, namely MACS0416 and MACS1206, as part of the analysis published in Olave-Rojas et al. 2018. In this case, we used: 1) ISOMER to select cluster members, 2) the DS-Test to verify the existence of substructures in the clusters and to verify the kinematic deviation of each galaxy from the main cluster, and 3) LAGASU to assign galaxies to different substructures (see Figure 2 in Olave-Rojas et al. 2018). We found more substructures in the outer part ($r \geq r_{200}$) of the clusters than in the inner regions ($r < r_{200}$). These results agree with the results reported by other authors for these clusters (see Biviano et al. 2013, Balestra et al. 2016). We note that with CALSAGOS, we are able to recover the ‘‘Sext’’ structure identified by (Balestra et al. 2016) in MACS0416.

In particular, for MACS0416 Balestra et al. 2016 found 781 spectroscopic members and a velocity dispersion of $\sigma_{cl} = 996_{-16}^{+12}$ km s⁻¹, and these authors report a spectroscopic completeness that varies between 0.5 and 0.7 decreasing from the inner to the outer regions of the cluster. If we select the cluster members using ISOMER, we obtain 890 ± 53 spectroscopic members and a velocity dispersion of $\sigma_{cl} = 1101 \pm 22$ km s⁻¹. Our estimation of the veloc-

ity dispersion is consistent within 1σ with the result reported by Balestra et al. (2016). Furthermore, when we select the cluster members using CLUMBERI we obtain 1036 ± 10 spectroscopic members and a velocity dispersion of $\sigma_{cl} = 1036 \pm 10$ km s⁻¹. The velocity dispersion estimated with CLUMBERI differs by 9σ from the value reported in Balestra et al. (2016). However, we note that when we use CLUMBERI we find 32% more spectroscopic members than Balestra et al. (2016) and the velocity dispersion estimated with CLUMBERI is consistent within 2σ with the value estimated when we select the cluster members using ISOMER. Finally, it is important to note that the galaxies in the substructures of MACS0416 follow the same colour-magnitude relation as the whole cluster as was shown in Figure 3 of Olave-Rojas et al. (2018).

We also ran CALSAGOS in the cluster SpARCS J0035-4312 at $z = 1.34$ drawn from the GOGREEN sample. The results are shown in Figure 6 in which points with different colours correspond to galaxies in different substructures and grey points correspond to cluster members that are not part of a substructure. For this case, we have used the criterion that all groups/substructures within r_{200} from the cluster centre are considered as part of the principal halo.

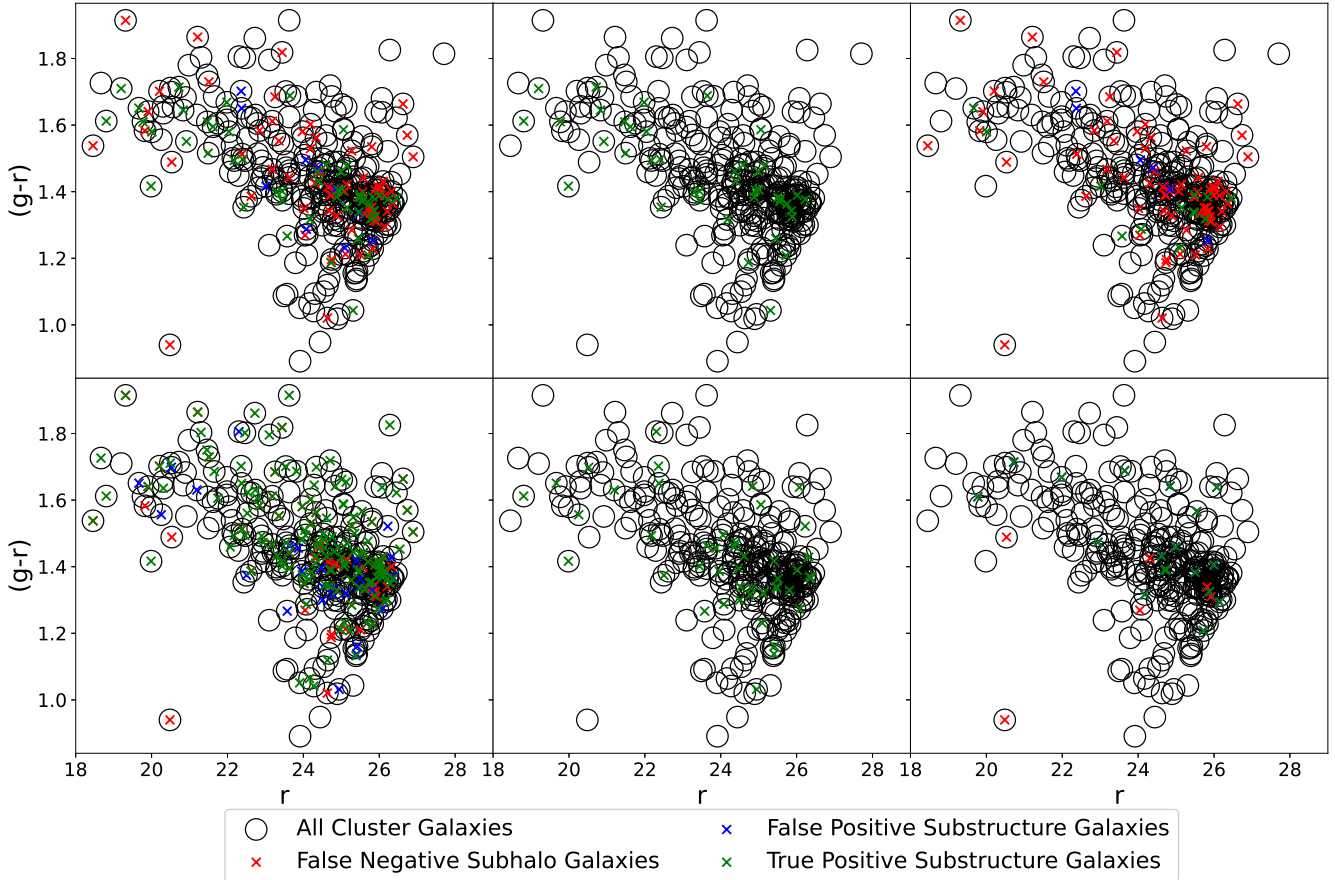


Figure 5. Colour–magnitude diagrams of the halo ID26. The colours are measured in the g and r S-PLUS broad bands (see Section 3.1). Cluster member galaxies are plotted with open black circles. Galaxies in false negative subhalos are plotted with red crosses, galaxies in false positive substructures are plotted with blue crosses and galaxies in true positive substructures are plotted with green crosses. In all panels the substructures were identified using LAGASU. In all top panels, the clusters members of halo ID26 which selected using CLUMBERI and in all bottom panels, the clusters members of halo ID26 which selected using ISOMER. Left panels: Identification of all substructures (inner and outer). Middle panels: identification of outer substructures (i.e. $r > r_{200}$). Right panels: identification of inner substructures (i.e. $r < r_{200}$)

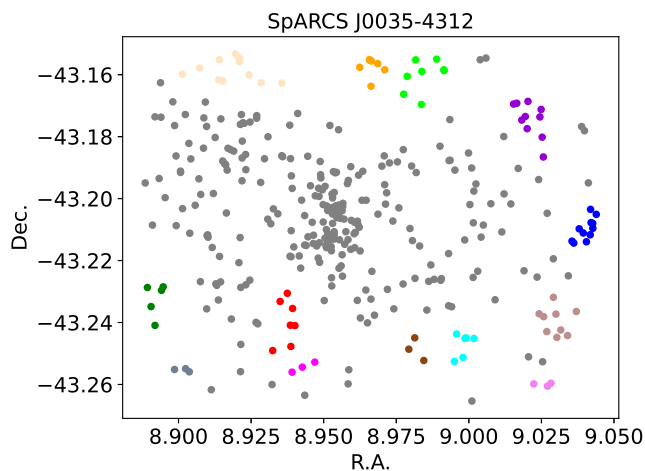


Figure 6. Substructure identification in the SpARCS J0035-4312 cluster at $z = 1.34$. Grey points correspond to galaxies in the principal halo of the cluster (i.e. galaxies that are cluster members but are not part of a substructure). Coloured points correspond to galaxies in different substructures.

4 DISCUSSION AND CONCLUSIONS

4.1 The importance of the clustering algorithms on the substructure analysis

Pre-processing has been demonstrated to be relevant in interpreting the results of galaxy evolution studies at low and high redshift (e.g. Li et al. 2012, Haines et al. 2015, Olave-Rojas et al. 2018, Reeves et al. 2021, Werner et al. 2022b). Thus, the study of galaxy properties in substructures and infalling groups in and around galaxy clusters is fundamental to constrain the importance of pre-processing in the quenching of star formation and structural transformations as well as investigate the links between galaxy evolution and the formation of large-scale structures. However, to carry out all these studies it is necessary to precisely identify the substructures and infalling groups in clusters of galaxies, especially at large cluster-centric distances ($r > r_{200}$).

There is no unique method to observationally search, find and identify substructures. For example, some authors use the projected phase-space diagram (e.g. Geller & Beers 1982, Biviano et al. 2013), the X-ray emission of the ICM (e.g. Briel et al. 1992, Bianconi et al. 2018), the kin-

matics of galaxies (e.g. Dressler et al. 2013, Hou et al. 2014), the density of the galaxies (e.g. Cybulski et al. 2014) or combined methods (e.g. Olave-Rojas et al. 2018, Lima-Dias et al. 2021). However, none of these methods can be considered the best and, in general, the performance of each method depends mainly on the kind of data, their quality, and the dynamical state of the clusters. In all the cases, the performance of a certain method improves when the statistics are high and when one considers parameter spaces with high dimensions (e.g. the performance improves when one adds redshifts to the positions of the galaxies) (Ramella et al. 2007, Tempel et al. 2017). Furthermore, as shown in Cohn (2012), substructures are less likely to be found in relaxed clusters than in merging clusters.

The majority of studies about pre-processing have so far been focused on the analysis of spectroscopic samples. This is mainly due to the fact that the methods used to search for substructures involve the derivation of peculiar velocities from the redshifts of the cluster members. The uncertainties of photometric redshifts are too high to derive peculiar velocities, and so methods such as the DS-test cannot be applied in these cases. However, this only allows the analysis of little samples of clusters (except in the case of the Local Cluster Substructure Survey, Haines et al. 2015) because spectroscopic observations are time-consuming, and the collection of a large spectroscopic sample demands large observing times, especially at high redshifts (e.g. Balogh et al. 2021).

On the other hand, it is less time-consuming to conduct deep imaging observations in different filters that allow large multi-band photometric samples to be built. One can thus estimate photometric redshifts by fitting an SED to the fluxes at different wavelengths, increasing the statistics in the redshift of the galaxies. However, photometric redshifts are less precise than spectroscopic redshifts, and this does not permit the application of the method based on the estimation of peculiar velocities in the detection of substructures. For this reason, the photometric surveys of galaxy clusters have been little explored in the study of pre-processing. Clustering represents, therefore, a technique that can be used as a tool to reliably search for substructures when there is little or no spectroscopic information available.

Clustering has been extensively used in astronomy to study the bimodality in the colour distribution of galaxies, to select cluster members or even to identify substructures. Among the most used algorithms there are the Kaye’s Mixture Model (KMM, Ashman et al. 1994) and the Gaussian Mixture Model (GMM, Muratov & Gnedin 2010). Both algorithms group galaxies assuming that their distribution in position, redshift or colour is better represented by a collection of n Gaussians rather than a single Gaussian. In this kind of algorithms the objects are assigned to groups according to their likelihood of membership. When we used Gaussian mixture methods to select substructures in and around galaxy clusters we noted that all the galaxies were assigned to one group that corresponded to the main cluster. This means that the algorithm would attribute galaxies that are not part of the same structure for their peculiar velocities and positions to the same group (e.g. Jaffé et al. 2013, Olave-Rojas et al. 2018).

When we use photometric redshifts, this can be an even

bigger problem due to the errors on the redshift estimation. In this case it is better to use clustering algorithms based on density of points to identify substructures. For this reason, it is necessary to use combined clustering algorithms or at least to select the best clustering algorithm to our purpose and test its performance in a sample with a known substructure list.

4.2 Strengths and limitations of CALSAGOS

We observe that the selection with ISOMER has greater uncertainty than the selection with CLUMBERI. This could be due to the fact that ISOMER was developed to select spectroscopic cluster members. Indeed, on one hand we assumed a certain shape of the gravitational profile to use the escape velocity for the selection of cluster members, and on the other hand, when we use spectroscopic redshifts we always select fewer cluster members because sampling is always partial (e.g. see the spectroscopic observational strategies in Biviano et al. 2013 and Balestra et al. 2016). In this sense, we can say that ISOMER selects cluster members more conservatively than CLUMBERI. However, ISOMER gives us a selection with less contamination than CLUMBERI.

Furthermore, when we use LAGASU to identify substructures in clusters we note that DBSCAN searches for groups without distinguishing between the principal cluster and the substructures. This means that when we run LAGASU over the galaxy cluster, the central part of the cluster (i.e. the principal halo in the mock) is also selected as a group within the sample. This is because DBSCAN does not receive in input any information about the dynamics of the galaxy cluster. For this reason, we have decided to add two criteria: 1) when we use a spectroscopic sample, the group that is nearest to the central position and redshift of the cluster corresponds to the main cluster, and the rest of the identified groups are considered as substructures, and 2) when we use photometric samples, all groups in the central part of the cluster (i.e. within r_{200}) are considered as part of the principal halo.

To quantify the precision of CALSAGOS in the detection and mapping of galaxy cluster substructures in observational data, we ran the package in a region of the mock catalogue without considering the information about the membership of the galaxies to the subhalos. When we consider all substructures (inner and outer) we obtain a F_1 -score of 0.5 and, precision of 75% and a completeness of 40%. The low value of the F_1 -score is not necessarily due to a failure in the package, but rather to its limitations, because LAGASU assigns galaxies to each substructure by using the two-dimensional position of the galaxies (R.A. and Dec.) and the number density. This produces a high number of false negatives, i.e. the program does not find a high number of substructures that are in fact subhalos in the mock. Interestingly, the majority of these false negatives are in the inner part of the halo where projection effects may affect more the detection of substructure and so LAGASU does not resolve them.

When we only consider the outer substructures (i.e. $r > r_{200}$) we obtain a F_1 -score of 0.8, a precision of 85% and a completeness of 100%. In particular, 85% of the identifications are true positive and 0% of the subhalos are false negative. When we only consider inner substructures (i.e. $r \leq r_{200}$) the F_1 -score drops to 0.4. This value is a result of the fact that 70% of the identified subhalos are false nega-

tive. Nevertheless, 80% of our identifications are true positives. Therefore, the low performance in the inner part of the cluster is a result of the fact that in this region the substructures overlap with the main cluster, generating a projection effect and the consequent confusion between the main cluster and the substructures. This effects is less important in the cluster outskirts and, as a result, the performance of LAGASU increases when we only consider the outer substructures. Besides, due to physical mechanisms within the cluster core, internal groups and substructures are more likely to be destroyed and are thus more difficult to detect (Vijayaraghavan & Ricker 2013; Jaffé et al. 2013).

The above results are obtained independently of the method used for the selection of cluster members (ISOMER or CLUMBERI), and we also obtain the same results when we select a halo from the mock and only run LAGASU over it. Besides, it is important to note that the methods used with observational data to search, find and identify substructures differ from those used in numerical simulations. In the case of the observational data, the substructure is defined in terms of position and kinematic. In the case of numerical simulations, the galaxies that belong to a subhalo must be gravitationally bound to one another. Thus, if CALSAGOS identifies a substructure in a catalogue from a cosmological simulation in which the subhalos are known, this may not always correspond to a subhalo.

According to the results of the F_1 -score, it can be concluded that the method presented in this paper has a residual intrinsic bias that has to be taken into account whenever CALSAGOS is used to select cluster members and substructures. In particular, we cannot obtain most of the information on the substructures that are closer to the cluster centre in observational data. However, the projected information in two dimensions tells us about the distribution of galaxies in the cluster, and we note that a substructure in the cluster could or not fall into a selected group by the clustering algorithms.

The results obtained from the detailed analysis of halos ID4 and ID5 show that CALSAGOS is not able to distinguish clusters that are in the process of merging. However, if we treated these systems as one we can reach a F_1 -score of 0.6, a precision of 70% and a completeness of 50%. The F_1 -score is above the median value obtained for the entire sample considering all the substructures (see Section 3.4), the precision is below the median and the completeness is above the median.

Figure 4 and the results of the KS test demonstrate that our method for cluster member selection and substructure identification do not introduce biases in colour and apparent magnitude. Thus, the mock galaxies have statistically indistinguishable colour distributions regardless of being cluster, subhalo or substructure members. On the other hand, Figure 5, together with the results of the KS test, shows that mock galaxies in all, outer or inner identified substructures have the same $(g-r)$ colour distribution of the mock galaxies in the entire cluster. Furthermore, we note that the galaxies in the false negative subhalos, false positive and true positive substructures follow the same distribution as the cluster members in the CMD. This result is also corroborated by the results of the KS test. According to this, we can conclude that CALSAGOS does not introduce colour or magnitude de-

pendent biases both in the selection of cluster members and in the identification of substructures.

On the other hand, Table 2 shows that the precision of CALSAGOS in the substructures identification depends on the quality of the cluster member selection and the type of redshift: if we use photometric redshifts to select cluster members, the precision is lower than when using z_{spec} . On the other hand, the completeness tends to be better when we use z_{phot} because more galaxies are selected as cluster members.

In spite of the fact that we used the S-PLUS mock catalogues to test the performance and accuracy of CALSAGOS, we want to remark that this package was also successfully employed in observational data of clusters of galaxies at intermediate and high redshift to search, find and identify substructures within and around galaxy clusters as we show in Section 3.4.1. Thus this paper demonstrates that CALSAGOS can be used on real or mock data to reliably detect substructures in galaxy clusters and conduct studies on the pre-processing of galaxies.

5 SUMMARY

So far the majority of the observational works about the pre-processing and the properties of galaxies in the outer regions ($r \geq r_{200}$) of clusters have been developed on sparsely populated samples because they were focused on spectroscopic data. This is mainly due to the techniques used in the selection of cluster members and in the tools used to search for substructures. However, clustering algorithms are powerful tools that can be employed in the analysis of substructures in clusters of galaxies when only photometric redshifts or no redshifts are available. As shown in Olave-Rojas et al. (2018), this allows one to increase the statistics in these kinds of studies and to overcome the limitations of the spectroscopic samples.

For these reasons, the development of CALSAGOS offers an opportunity to extend the analysis of galaxy properties to the outer regions of clusters of galaxies by using photometric samples, because this is a tool based on clustering algorithms that has been tested on a mock galaxy sample which eliminates the problem of the dependence on spectroscopic data.

We find that the DBSCAN algorithm used in LAGASU provides a reliable detection of the cluster substructures. In particular we find that LAGASU has a better performance when identifying substructures in the outer regions of the cluster ($r \geq r_{200}$) reaching a F_1 -score of 0.8, a precision of 85% and a completeness of 100%. When we consider all the substructures the F_1 -score, the precision and the completeness drop to 0.5, 70% and 40%, respectively. We attribute this to the fact that in the inner regions of the clusters it is more likely to have several substructures along the same line of sight. As a result, LAGASU, which works in two dimensions, cannot resolve them because they appear as the same substructure in projection. This is the main limitation of CALSAGOS.

We must keep in mind that we probe the performance of an observational method to search, find and identify substructures over a mock catalogue in which we have subhalos that were defined according to their gravitational potential.

However, when one only works with photometric samples in which no spectroscopic redshift is available, the information on the dynamics of the galaxies in a cluster cannot be obtained. So LAGASU works without prior knowledge of the dynamics of the cluster, and this means that the substructures that are identified may not correspond to systems with internal dynamics that differ from those of the principal cluster.

ACKNOWLEDGEMENTS

We thank the anonymous referee for the helpful and constructive feedback. We especially thank Claudia Mendes de Oliveira the P.I. of the Southern Photometric Local Universe Survey (S-PLUS) for giving us access to the mock catalogues to test this package. We are also grateful to Ricardo Demarco, Yara Jaffé, and Diego Pallero for their input on this project. Besides, we would like to thank everyone who has tested CALSAGOS extensively and provided us with invaluable feedback. PA-A thanks Coordenação de Aperfeiçoamento de Pessoal de Nível Superior (CAPES) for supporting his PhD scholarship (project 88887.596140/2020-00)

DATA AVAILABILITY

CALSAGOS can be downloaded from the webpage <https://github.com/dolaver/calsagos> that also contains the working tutorial `test.py`. Besides, the mock catalogue used in this work is available upon request from Pablo Araya-Araya (e-mail: paraya-araya@usp.br).

REFERENCES

Angulo R. E., White S. D. M., 2010, *MNRAS*, **405**, 143
 Araya-Araya P., Vicentin M. C., Sodr e Laerte J., Overzier R. A., Cuevas H., 2021, *MNRAS*, **504**, 5054
 Arnouts S., Cristiani S., Moscardini L., Matarrese S., Lucchin F., Fontana A., Giallongo E., 1999, *MNRAS*, **310**, 540
 Ashman K. M., Bird C. M., Zepf S. E., 1994, *AJ*, **108**, 2348
 Bah e Y. M., McCarthy I. G., Balogh M. L., Font A. S., 2013, *MNRAS*, **430**, 3017
 Balestra I., et al., 2016, *ApJS*, **224**, 33
 Balogh M. L., et al., 2021, *MNRAS*, **500**, 358
 Beers T. C., Flynn K., Gebhardt K., 1990, *AJ*, **100**, 32
 Bianconi M., Smith G. P., Haines C. P., McGee S. L., Finoguenov A., Egami E., 2018, *MNRAS*, **473**, L79
 Biviano A., Rosati P., Balestra I., et al. 2013, *A&A*, **558**, A1
 Briel U. G., Henry J. P., Boehringer H., 1992, *A&A*, **259**, L31
 Cerulo P., et al., 2016, *MNRAS*, 457, 2209
 Cerulo P., et al., 2017, *MNRAS*, **472**, 254
 Chabrier G., 2003, *PASP*, **115**, 763
 Chiang Y.-K., Overzier R., Gebhardt K., 2013, *The Astrophysical Journal*, **779**, 127
 Clay S. J., Thomas P. A., Wilkins S. M., Henriques B. M. B., 2015, *MNRAS*, **451**, 2692
 Cohn J. D., 2012, *MNRAS*, **419**, 1017
 Couch W. J., Barger A. J., Smail I., Ellis R. S., Sharples R. M., 1998, *The Astrophysical Journal*, **497**, 188
 Cybulski R., Yun M. S., Fazio G. G., Gutermuth R. A., 2014, *Monthly Notices of the Royal Astronomical Society*, **439**, 3564
 De Lucia G., Blaizot J., 2007, *MNRAS*, **375**, 2

Demarco R., et al., 2010, *ApJ*, **725**, 1252
 Dempster A. P., Laird N. M., Rubin D. B., 1977, *JOURNAL OF THE ROYAL STATISTICAL SOCIETY, SERIES B*, **39**, 1
 Diaferio A., 1999, *MNRAS*, **309**, 610
 Dressler A., 1980, *ApJ*, **236**, 351
 Dressler A., Shectman S. A., 1988, *AJ*, **95**, 985
 Dressler A., Smail I., Poggianti B. M., Butcher H., Couch W. J., Ellis R. S., Oemler Jr. A., 1999, *ApJS*, **122**, 51
 Dressler A., Oemler Jr. A., Poggianti B. M., Gladders M. D., Abramson L., Vulcani B., 2013, *ApJ*, **770**, 62
 Ester M., Kriegel H.-P., Sander J., Xu X., 1996, in *Proceedings of the Second International Conference on Knowledge Discovery and Data Mining, KDD'96*. AAAI Press, pp 226–231, <http://dl.acm.org/citation.cfm?id=3001460.3001507>
 Fakhouri O., Ma C.-P., Boylan-Kolchin M., 2010, *Monthly Notices of the Royal Astronomical Society*, **406**, 2267
 Finn R. A., et al., 2005, *ApJ*, **630**, 206
 Fujita Y., 2004, *PASJ*, **56**, 29
 Geller M. J., Beers T. C., 1982, *PASP*, **94**, 421
 Gobat R., Rosati P., Strazzullo V., Rettura A., Demarco R., Nonino M., 2008, *A&A*, **488**, 853
 Haines C. P., et al., 2015, *ApJ*, **806**, 101
 Harrison E. R., 1974, *ApJ*, **191**, L51
 Henriques B. M. B., White S. D. M., Thomas P. A., Angulo R., Guo Q., Lemson G., Springel V., Overzier R., 2015, *MNRAS*, **451**, 2663
 Hodges J. L., 1958, *Arkiv f r Matematik*, **3**, 469
 Hou A., et al., 2012, *MNRAS*, **421**, 3594
 Hou A., Parker L. C., Harris W. E., 2014, *Monthly Notices of the Royal Astronomical Society*, **442**, 406
 Ilbert O., et al., 2006, *A&A*, **457**, 841
 Jaff e Y. L., Poggianti B. M., Verheijen M. A. W., Deshev B. Z., van Gorkom J. H., 2013, *MNRAS*, **431**, 2111
 Jaff e Y. L., et al., 2016, *MNRAS*, **461**, 1202
 Just D. W., et al., 2019, *ApJ*, **885**, 6
 Kauffmann G., White S. D. M., Heckman T. M., M nard B., Brinchmann J., Charlot S., Tremonti C., Brinkmann J., 2004, *MNRAS*, **353**, 713
 Kitzbichler M. G., White S. D. M., 2007, *MNRAS*, **376**, 2
 Kolmogorov A. L., 1933, *G. Ist. Ital. Attuari*, **4**, 83
 Lewis I., et al., 2002, *MNRAS*, **334**, 673
 Li I. H., Yee H. K. C., Hsieh B. C., Gladders M., 2012, *ApJ*, **749**, 150
 Lima-Dias C., et al., 2021, *MNRAS*, **500**, 1323
 Maraston C., 2005, *MNRAS*, **362**, 799
 McGee S. L., Balogh M. L., Bower R. G., Font A. S., McCarthy I. G., 2009, *MNRAS*, **400**, 937
 Mendes de Oliveira C., et al., 2019, *MNRAS*, **489**, 241
 Molino A., et al., 2020, *MNRAS*, **499**, 3884
 Muratov A. L., Gnedin O. Y., 2010, *ApJ*, **718**, 1266
 Olave-Rojas D., Cerulo P., Demarco R., Jaff e Y. L., Mercurio A., Rosati P., Balestra I., Nonino M., 2018, *MNRAS*, **479**, 2328
 Peng Y.-j., et al., 2010, *ApJ*, **721**, 193
 Planck Collaboration et al., 2014, *A&A*, **571**, A16
 Poggianti B. M., Smail I., Dressler A., Couch W. J., Barger A. J., Butcher H., Ellis R. S., Oemler Jr. A., 1999, *ApJ*, **518**, 576
 Poggianti B. M., von der Linden A., De Lucia G., et al. 2006, *ApJ*, **642**, 188
 Postman M., et al., 2005, *The Astrophysical Journal*, **623**, 721
 Press W. H., Schechter P., 1974, *ApJ*, **187**, 425
 Press W. H., Teukolsky S. A., Vetterling W. T., Flannery B. P., 2007, *Numerical Recipes 3rd Edition: The Art of Scientific Computing*, 3 edn. Cambridge University Press, New York, NY, USA
 Rahmah N., Sitanggang I. S., 2016,

- IOP Conference Series: Earth and Environmental Science, 31, 012012
- Ramella M., et al., 2007, *A&A*, 470, 39
- Reeves A. M. M., et al., 2021, *MNRAS*, 506, 3364
- Schwarz G., 1978, *The Annals of Statistics*, 6, 461
- Shamshiri S., Thomas P. A., Henriques B. M., Tojeiro R., Lemson G., Oliver S. J., Wilkins S., 2015, *MNRAS*, 451, 2681
- Smirnov N., 1948, *The Annals of Mathematical Statistics*, 19, 279
- Springel V., et al., 2005, *Nature*, 435, 629
- Tempel E., Tuvikene T., Kipper R., Libeskind N. I., 2017, *A&A*, 602, A100
- Van Rijsbergen C. J., 1979, *Information Retrieval*, 2nd edn. Butterworth-Heinemann, USA
- Vijayaraghavan R., Ricker P. M., 2013, *MNRAS*, 435, 2713
- Werner S. V., et al., 2022a, *MNRAS*,
- Werner S. V., Hatch N. A., Muzzin A., van der Burg R. F. J., Balogh M. L., Rudnick G., Wilson G., 2022b, *MNRAS*, 510, 674
- West M. J., Bothun G. D., 1990, *ApJ*, 350, 36
- Xu S.-k., Wang C., Zhuang L.-h., Gao X.-h., 2019, *Chinese Astron. Astrophys.*, 43, 225
- Yahil A., Vidal N. V., 1977, *ApJ*, 214, 347
- Zabludoff A. I., Mulchaey J. S., 1998, *ApJ*, 496, 39
- van der Burg R. F. J., et al., 2020, *A&A*, 638, A112

This paper has been typeset from a $\text{\TeX}/\text{\LaTeX}$ file prepared by the author.